Journal of Volcanology and Geothermal Research 349 (2018) 74–82

Contents lists available at ScienceDirect

Journal of Volcanology and Geothermal Research

journal homepage: www.elsevier.com/locate/jvolgeores

Induced thermoluminescence as a method for dating recent volcanism: Hawaii County, Hawaii, USA

Derek W.G. Sears [a,*], Hazel Sears [a], Alexander Sehlke [b], Scott S. Hughes [c]

[a] NASA Ames Research Center, Bay Area Environmental Research Institute, Mountain View, CA 95035, USA
[b] NASA Ames Research Center, Mountain View, CA 95035, USA
[c] Geosciences Department, Idaho State University, Pocatello, ID 83209, USA

ARTICLE INFO

Article history:
Received 5 April 2017
Received in revised form 25 September 2017
Accepted 27 September 2017
Available online 30 September 2017

Keywords:
Thermoluminescence
Basalts
Volcanoes
Crystallization
Hawaii

ABSTRACT

We have measured the induced thermoluminescence (TL) properties of fifteen samples of basalts collected from the Big Island of Hawaii in order to continue our investigation into the possible utility of this technique as a chronometer. Previous studies of basalts from Idaho have suggested the induced TL of basalts increases with age. Meteorite data suggest two possible explanations for this observation which are that (1) the initial glassy or amorphous phases crystalize with time to produce feldspar, the mineral producing the TL signal, and (2) feldspars lose Fe as they equilibrate and since Fe is a quencher of TL this would cause an increase in TL. The old basalts from Kohala (>100 ka), which are mostly alkali basalts, have TL sensitivities 10–100 times higher than the much younger tholeiites from Kilauea and Mauna Loa (<50 ka). The thermoluminescence of feldspars is strongly dependent on composition and when this is corrected for, using literature data, the slope of the regression line for the plot of log TL sensitivity against historic or radiometric age for the Hawaii basalts is within 2 sigma of the regression line for the analogous plot for the Idaho basalts, although the Hawaii line is much shallower (0.0015 ± 0.0012 for Hawaii cf. 0.0039 ± -0.0014 for Idaho, 2σ uncertainties). However, the intercepts are significantly different (0.78 ± 0.18 for Hawaii cf. -0.079 ± 0.28 for Idaho, 2σ uncertainties). These results suggest that TL sensitivity has the potential to be a means of dating volcanism in the 0–800 ka range, although the scatter in the data – especially for the <50 ka samples – needs to be understood, and a means found for its removal, before the technique has the possibility of being practically useful.

1. Introduction

Thermoluminescence (TL), or one of the several closely related techniques, is in routine use for dating pottery and quaternary sediments (Aitken, 1985, 1999). A great many papers have been published exploring the use of natural TL measurements for dating volcanism and while many report success (e.g. May, 1977, 1979; Guérin and Valladas 1980; Berger, 1991), there is also a widely known problem that many volcanic rocks display "anomalous fading" (Wintle, 1973), which makes the technique unreliable. Many attempts to circumvent the difficulties have been reported (e.g. Guérin and Valladas 1980; Berger, 1991), but none have been universally accepted and the technique has yet to become widely adopted by volcanologists.

Natural TL is the "as received" TL signal. It results from the excitation of electrons to metastable sites in a crystal by ionizing radiation that has passed through the crystal. The source of the radiation is mostly internal radioactivities in the rock and surroundings, but cosmic rays may also contribute. Once trapped in these excited states, the electrons can build up in a manner related to time and dose rate. When the electrons are released by heating the sample, the electrons return to the ground state through "luminescence centers" producing light. Thus the thermoluminescence signal is proportional to absorbed dose and can be converted to the actual dose absorbed using a laboratory calibration technique. In turn, this dose can be divided by dose rate, measured directly in the field or calculated from the composition of the sample, to obtain an age. A nice example of the process is given by Sutton (1985) in his dating of the Meteor Crater.

In the late seventies May (1977, 1979) reported his attempt to date the volcanism on the Big Island of Hawaii using natural thermoluminescence. The results he obtained were in reasonable agreement with historic dates and ages obtained by radiometric dating. However, his data also showed an intriguing relationship between the "artificial TL" and age and it is that which we explore here.

The "artificial TL", better termed "induced TL", is the level of the TL that can be induced in a sample by removal of its natural signal, by heating to 500 °C for example, and then exposing the sample to a standard dose in the laboratory. The level of induced TL depends on the amount and nature of the mineral responsible for the TL signal, rather than dose rate. In most igneous rocks this mineral responsible for the TL

* Corresponding author.
E-mail address: derek.sears@nasa.gov (D.W.G. Sears).

https://doi.org/10.1016/j.jvolgeores.2017.09.022
0377-0273/

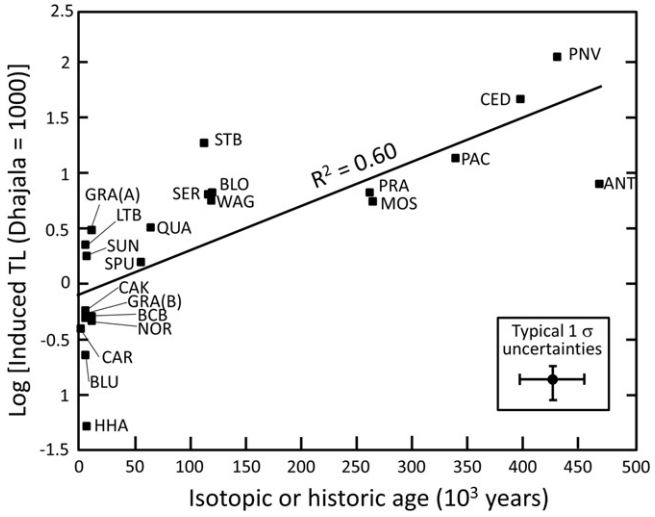

Fig. 1. Logarithm of the induced TL (composition corrected) against age for samples of basalt from the eastern Snake River Plain, Idaho. (The plot is from Sears et al., 2017 corrected for a factor-of-four error in the TL values and updated with improved data for a few samples). The typical uncertainties were visually assessed from fig. 5 of the Sears et al. (2017) paper and apply to samples >50 ka, for younger samples the uncertainties are much smaller, usually about the size of the symbol).

signal is feldspar. Mineral separations show that among the common rock-forming minerals the induced TL of feldspar is at least 13 times that of the other minerals (Lalou et al., 1970). This is confirmed by cathodoluminescence images where the luminescence is a result of electron bombardment (Akridge et al., 2004).

Any process that affects the feldspar affects the induced TL. For example, ordinary chondrite meteorites show a range of 10^5 in their induced TL which reflects the level of metamorphism that they have experienced (Sears et al., 1980, 2013). Metamorphism causes the feldspathic glass, which is initially present, to crystalize so that induced TL measurements are one of the best ways of quantitatively estimating the degree of crystallization and thereby the relative levels of metamorphism experienced by individual meteorites. The classification scheme based on induced TL measurements became an established part of meteorite classification. A very different example is basaltic meteorites, the eucrites, which are understood to come, with their close relatives the diogenites and howardites, from the asteroid Vesta (McCord et al., 1970; Drake, 2001). Their induced TL increases by a factor of 100 with the levels of metamorphism they have experienced which can be tracked by the heterogeneity of the pyroxenes (Batchelor and Sears, 1991a, 1991b). In this case, the little-metamorphosed meteorites have plenty of crystalline feldspar but the low levels of induced TL are due to the presence of Fe^{2+} in the feldspar. This ion is a thermoluminescence quencher. However, with increasing levels of metamorphism the Fe^{2+} diffuses out of the feldspar (and into the pyroxene) and the induced TL intensity increases (Sears, 2015).

Both these mechanisms, formation of crystals from glass and diffusion of Fe out of the feldspar, could occur in basalts. Basalts are non-equilibrium systems. They are formed rapidly from the melt so much of the feldspathic elements are glassy or amorphous and the feldspars that are present will contain incompatible elements like Fe. It seems reasonable to hypothesize that both these processes are operative in basalts and would cause induced TL to increase with time and therefore provide a chronometer.

With these ideas in mind, Sears et al. (2017) recently performed a study of the induced TL of 24 basalts from the eastern Snake River Plain in Idaho (Fig. 1). The ages of the basalts ranged from 2 ka to 470 ka and the induced TL increased by an order of magnitude in about 400 ka. However, there was considerable scatter that is only partially understood. In the present paper, we are interested in (1) confirming May's observation that Hawaiian basalts show a trend for increasing induced TL, (2) seeing if the correlation obtained from the Hawaii samples is the same as the correlation observed for the Idaho basalts, and (3) looking for additional clues as to the cause of the scatter in the TL-age relationship and ways to remove it.

2. Experimental methods

2.1. Sample collection

Fifteen samples were obtained from flows from the Kohala, Mauna Loa and Kilauea volcanoes. Eleven were sites previously sampled by May (1977, 1979), where further details can be found. May used the same samples as those used for radiometric dating (Table 1). In addition to the sites at which May sampled, we obtained four samples from Mauna Loa lava flows (Wolfe and Morris, 1996). Thus we collected three Kilauea samples, six Mauna Loa samples, and six Kohala samples. The locations are shown on a map in Fig. 2 and the samples listed with ages in Table 1.

2.2. Thermoluminescence measurements

Our methods for determining the TL properties of the basalts were recently described by Sears et al. (2017) and the theory and measurement of the TL properties of meteorites and lunar samples were described by Sears et al. (2013). We will therefore only briefly summarize the procedure here.

Samples were gently crushed in stainless steel and agate pestles and mortars to pass through a 250 μm sieve (enough to pour like

Table 1
Samples used in the present study, their locations, their ages (with references) and descriptions, in order of increasing age.

Sample	Volcano	Long. (W)	Lat. (N)	Age (ka)	Ref[a]	Description[b]
May-12	Kilauea	154.83758	19.50765	0.075	a	Puna series (tholeiite)
May-15	Kilauea	154.94515	19.43569	0.085	a	Puna series (tholeiite)
May-30	Mauna Loa	155.89315	19.89425	0.156	a	Kau series (tholeiite)
May-50	Kilauea	154.96410	19.37173	0.265	a	Puna series (tholeiite)
MLO-295	Mauna Loa	155.46482	19.21449	1.3 ± 0.1	f	Kau series (tholeiite)
MLO-383	Mauna Loa	155.48132	19.18536	3.5 ± 0.1	f	Kau series (tholeiite)
May-24	Mauna Loa	155.62133	19.06738	3.74 ± 0.15	d, e	Kau series (tholeiite)
MLO-637	Mauna Loa	155.51050	19.14985	3.9 ± 0.1	f	Kau series (tholeiite)
MLO-540	Mauna Loa	155.48383	19.18280	8.0 ± 0.1	f	Kau series (tholeiite)
May-35	Kohala	155.76187	20.07590	140 ± 4	b	Hawi series (AB/trachyte)
May-36	Kohala	155.76310	20.07982	153 ± 7	b	Hawi series (AB/hawaiite)
May-41	Kohala	155.87587	20.10915	181 ± 3	c	Hawi series (AB/mugearite)
May-42	Kohala	155.85468	20.07230	184 ± 3	c	Hawi series (AB/mugearite)
May-33	Kohala	155.70710	20.03423	196 ± 7	b	Hawi series (AB/hawaiite)
May-37	Kohala	155.89687	20.18680	400 ± 8	c	Pololu series (Tholeiite)

[a] References for ages: a, Historic flows; b, McDougall (1969); c, McDougall and Swanson (1972); d, Rubin and Corrine (1960); e, Sullivan et al. (1970); f, Wolfe and Morris (1996).
[b] Series and descriptions from May (1979) and Wolfe and Morris (1980). AB indicates alkali basalt.

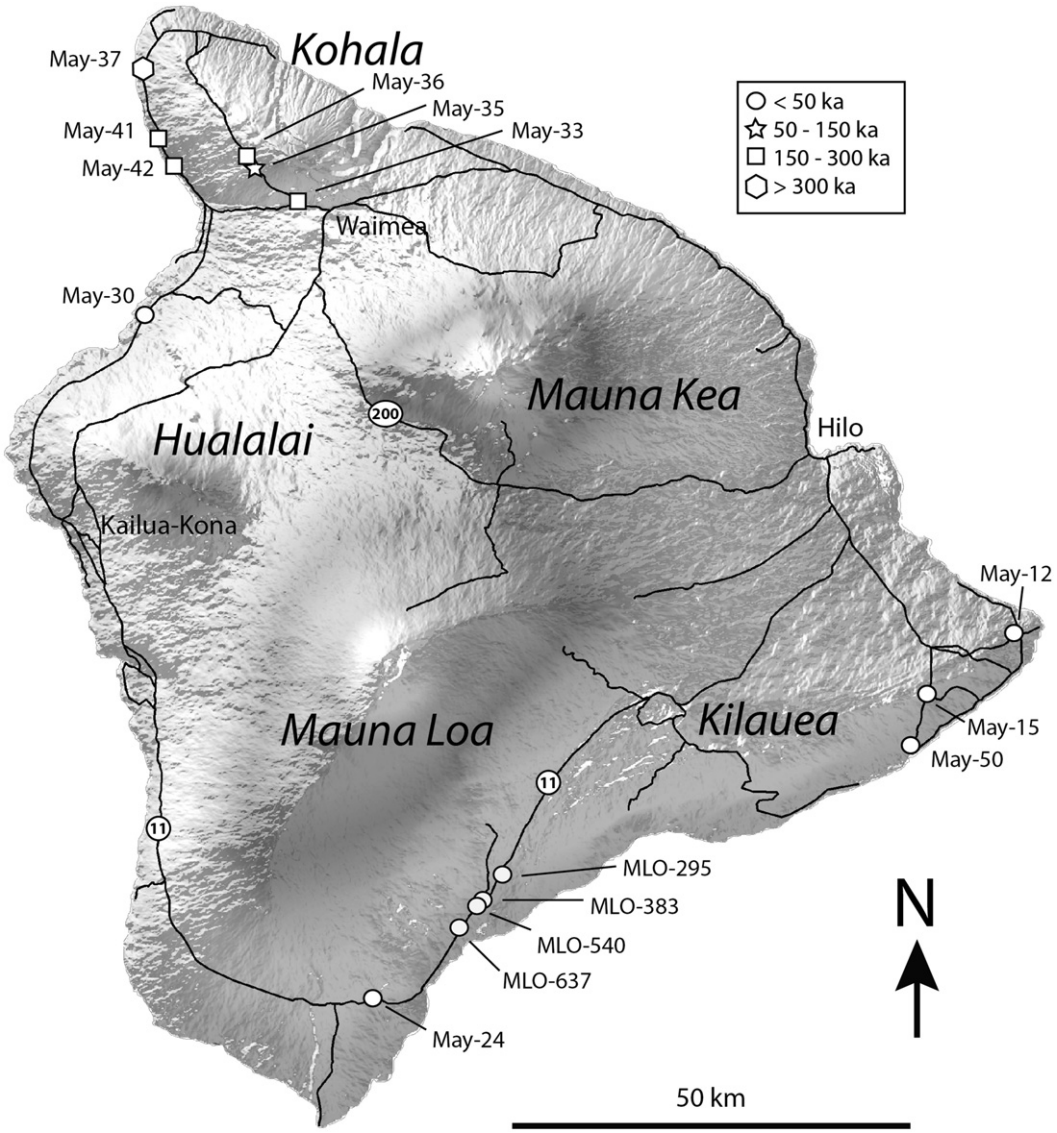

Fig. 2. Map showing locations at which samples were collected for the present study. The symbols reflect age (see key).

sand and not fine enough to clump like flour). Four milligram aliquots were then taken for TL measurement, enough to fill a 5 mm diameter, 2 mm deep, pan with a monolayer of powder. The pan was then placed in modified commercial Daybreak Nuclear and Medical Inc. thermoluminescence apparatus. Five glow curves (light produced versus heating temperature from room temperature to 500 °C) were recorded for each sample, one curve for powder in the natural state, three after exposure to a standard dose of beta radiation, and one in the drained state. The purpose of the last curve was to record the background signal and the black body radiation from the sample. The Dhajala meteorite was used to check the stability of the apparatus and act as normalization standard to aid interlaboratory comparison.

2.3. Petrography

Clean 1–2 cm chips of our samples were sent to National Petrographic Services Inc., Houston, Texas, for the preparation of impregnated polished thin sections. Each sample was examined under a Zeiss Orthoplan optical microscope in plain transmitted light and with crossed polars. The modal abundance of glass, microlites, phenocrysts, and olivine were measured from the transmitted light images using the Adobe Photoshop image analysis software.

2.4. Geochemistry and chronology

Literature data were used to obtain compositions and ages for our samples. The collection sites for our samples were located on the geological map of Wolfe and Morris (1996) and the geological unit noted. From this, the compilation of compositional and chronological data for the unit in the brochure that accompanied the map was used to obtain compositions and ages for our samples.

3. Results

3.1. Thermoluminescence results

Our thermoluminescence data are listed in Table 2. Representative and atypical glow curves are shown in Fig. 3. The three representative samples are spread across the age – composition matrix; #37 is an old tholeiite, #30 is a young tholeiite and #33 is intermediate age alkali basalt. There are subtle differences between these curves but in general they show the presence of four or five peaks giving a broad but

Table 2
Thermoluminescence data for the present samples in order of increasing age.

Sample	TL sensitivity[a]	Peak positions (°C)[b]					HT/LT[c]
	(Dhajala = 1000)	1	2	3	4	5	
May-12	2.8 ± 0.3	122	–	200	–	–	5.47 ± 0.79
May-15	3.0 ± 0.5	112	170		245	305	0.55 ± 0.02
May-30	6.3 ± 1.4	120	–	193	–	293	0.40 ± 0.07
May-50	3.3 ± 0.3	122	–	182	250	–	0.36 ± 0.07
MLO-295	0.07 ± 0.01	133	–	193	–	308	3.49 ± 0.25
MLO-383	7.7 ± 1.0	118	185	195	230	310	0.29 ± 0.03
May-24	3.5 ± 0.4	143	–	237	–	302	0.62 ± 0.09
MLO-637	3.8 ± 2.1	122	–	200	–	295	1.16 ± 0.55
MLO-540	3.8 ± 0.6	117	–	203	265	–	0.48 ± 0.10
May-35	42.3 ± 2.0	135	173	–	272	–	0.15 ± 0.06
May-33	235.4 ± 50.1	185	210	225	273	–	0.07 ± 0.01
May-36	55.4 ± 8.3	120	177	–	–	283	0.24 ± 0.02
May-41	30.5 ± 2.0	113	182	–	282		0.10 ± 0.02
May-42	82.5 ± 25.9	118	–	203	–	–	0.11 ± 0.02
May-37	15.0 ± 1.9	115	–	203	–	303	0.04 ± 0.01

[a] "TL sensitivity" is defined as the maximum induced TL level divided by the same value for the Dhajala meteorite. Uncertainties are standard deviations based on triplicate measurements.
[b] Positions of peaks in the TL glow curves or inflections indicative of unresolved peaks. Uncertainties on the peak positions can be visually estimated from Fig. 4 and are typically ~ ± 10 °C at the one sigma level.
[c] Ratio of the induced TL at ~325 °C to ~125 °C.

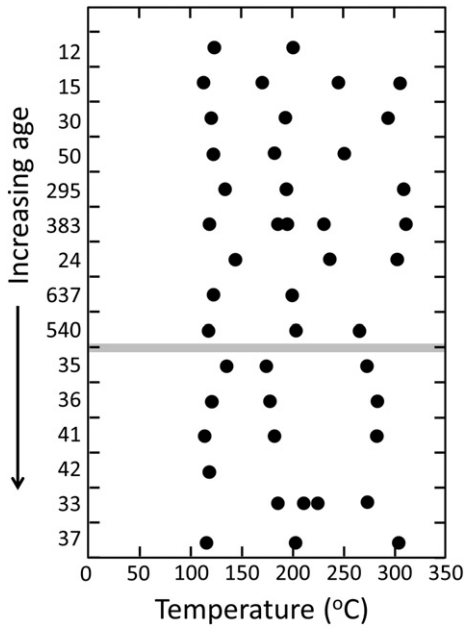

Fig. 4. Plot of peak positions for the present samples, identified on the y-axis by the digit portion of the sample name (see Table 1). The grey bar indicates the 20 ka separation for the samples, samples above the line are <20 ka, above are >20 ka). Although intensities vary considerable, certain peak temperatures appear to persist, i.e. ~120 °C, ~200 °C and ~300 °C. Similar behavior is observed for the Idaho basalts and all feldspar-bearing rocks.

somewhat hummocky band of TL that extends from 100 to 300 °C. In general they are very similar to the results of May for HI basalts and our previous results for ID basalts.

On the other hand, the three atypical curves are all low age tholeiites. Two (May-12 and MLO 295) have a single relatively high peak at ~300 °C, with only traces of the lower temperature peaks, while May-15 shows rather sharp peaks at ~100 °C and ~175 °C. This behavior indicates that the peaks in basalt TL curves are due to discrete minerals and not due to complex peak structures within a single mineral. For example, there could be compositionally discrete feldspars present and there could be low-temperature feldspar and high-temperature feldspar present. Based on our experience with meteorites, we suspect that the 100 °C peak is low-temperature feldspar, the ~200 °C peak is high-temperature feldspar while the ~300 °C peak is a Ca-rich feldspar. The peak positions (Fig. 4) indicate the persistence of these peak positions, keeping in mind that peak positions depend weakly on intensity and peak overlap. We return to this topic below when we discuss petrology and composition of our samples.

The thermoluminescence sensitivities for the present samples are plotted against the age of the samples in Fig. 5. The low age samples plot in a fairly tight cluster with TL in the range of 2.8 to 7.7 (Dhajala = 1000), excluding MLO-295 which is an outlier at 0.07. The five intermediate age samples spread but clearly have TL values an order of magnitude or more higher than the low age samples. The

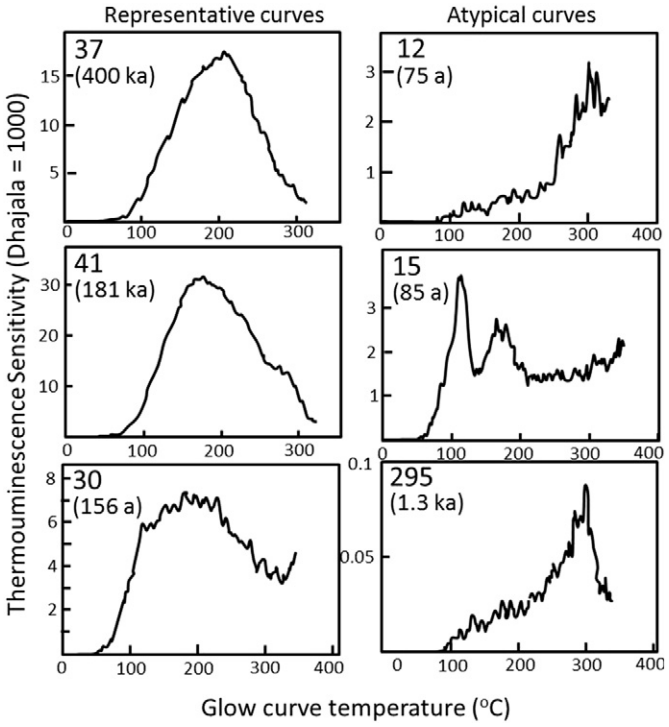

Fig. 3. Representative and atypical glow curves from the present study. The numbers refer to numerical part of the sample name (Table 1). The ages of the samples are also indicated but note that some are in years and some are in kiloyears.

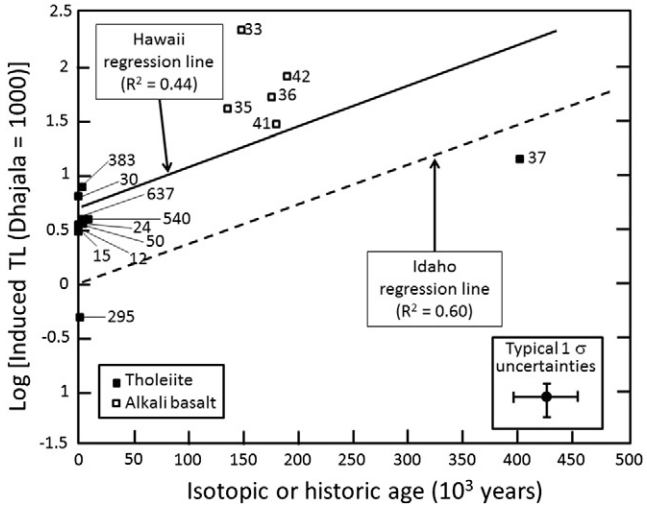

Fig. 5. Logarithm of the induced thermoluminescence level against the isotopic or historic age of the present samples. Tholeiites and alkali basalts are shown with different symbols as indicated in the key. Also shown are the regression lines through the present data (solid line) and through samples from the eastern Snake River Plain, Idaho (dashed line, Fig. 1). For typical uncertainties see the caption to Fig. 1.

oldest sample plots with TL value intermediate between the young and intermediate group. We also indicate on Fig. 5 the regression line and typical uncertainty bars for the present data and the regression line from our study of Idaho basalts. The data have not been weighted, raw data have been used, and no data have been rejected (see Appendix for details of data used in the regression analysis and the results). The Idaho regression line runs roughly parallel to the Hawaii line but displaced downwards by a factor of five. The uncertainty bars were determined by visual inspection of fig. 5 of the Sears et al. (2017) paper. Two points to note are (1) the vertical bar is asymmetric because the TL data are plotted on a logarithmic scale and the actual spread of data is normal; (2) to be conservative we have assumed the same uncertainties for the old Hawaiian K-Ar ages as the more modern Idaho K-Ar (actually Ar-Ar) ages. The Hawaiian uncertainties quoted in the literature are systematically one third to one half the modern uncertainties for the Idaho data.

3.2. Petrographic results

We reproduced images of our samples under transmitted light in Fig. 6, laid out in the pattern of data in the TL-age plot (Fig. 5). The trends observed are very similar to those observed for our Idaho study (Sears et al., 2017). The low-age samples are predominantly dark due to the abundance of opaque glass, with numerous large vesicles, while the older samples appear more crystalline with few or no vesicles. We expect some opaque oxides in the matrix as well, but these are hard to distinguish from the glass in the transmitted light microscopy.

The modal mineral abundances of our samples are listed in Table 3 and plotted in order of increasing age in Fig. 7. Microlites and glass show little systematic variation with age, although samples 12 and 15 are low in glass and sample 30 is low in microlites. Olivine abundance seems to show a decrease with increasing age. These results are unlike those for the Idaho basalts and indicate that we have not been able to identify any mineralogical trends that accompany aging although the low age basalts clearly have a much more opaque matrix than the older samples.

3.3. Compositional data

We made SiO_2 versus $Na_2O + K_2O$ plots for the units listed in Table 4 taking the compositional data from Wolfe and Morris (1996). Most of the geological units from which our samples came are compositionally homogeneous. The greatest spread was for unit hw whose SiO_2 and $Na_2O + K_2O$ values spread from 45.4 and 5.1 to 53.0 and 7.54 wt%. This corresponds to a range in normative anorthite content of An_{31} to An_{26}, not sufficient to significantly affect any of the present conclusions. The compositional data for our samples are plotted in the standard forms in Fig. 8. While the individual geologic units are relatively homogeneous, the different units show considerable compositional variation, from tholeiitic basalts of the Kilauea and Mauna Loa flows to mostly alkali-rich trachybasalts and trachyandesites of the Kohala flows.

Table 3
Modal abundance (vol%) of plagioclase phenocrysts, plagioclase microlites, olivine, and glass as determined by image analysis of transmitted light photo micrographs. Listed in order of increasing age[a].

Sample	$Plag_{pheno}$	$Plag_{micro}$	Olivine	Glass
May-12	0	38	21	41
May-15	5	58	10	27
May-30	0	9	20	71
May-50	0	26	0	73
MLO-295	0	45	0	54
MLO-383	0	31	7	62
May-24	0	32	9	59
MLO-637	0	39	10	51
MLO-540	0	24	14	62
May-35	0	38	3	59
May-36	0	36	4	60
May-41	0	42	4	54
May-42	0	33	2	65
May-33	0	50	2	48
May-37	0	34	4	62

[a] The given modal abundance is corrected for the presence of vesicles. Average uncertainty on abundance is ~5 vol%.

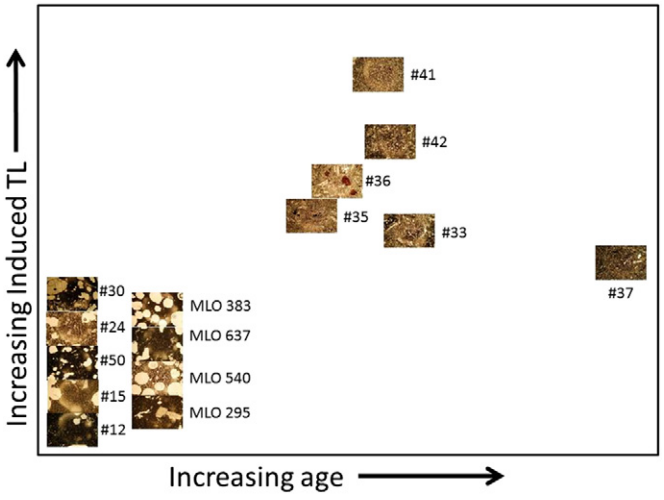

Fig. 6. Transmitted light photomicrographs of the thin sections of the samples in the present study laid out in the fashion of the induced thermoluminescence versus age plot (Fig. 5). The dark phase is glass and the lighter phase is crystalline. Numerous vesicles are present in the younger samples. The images and their changes with age are very similar to those observed for basalts from the Idaho volcanic system (Sears et al., 2017).

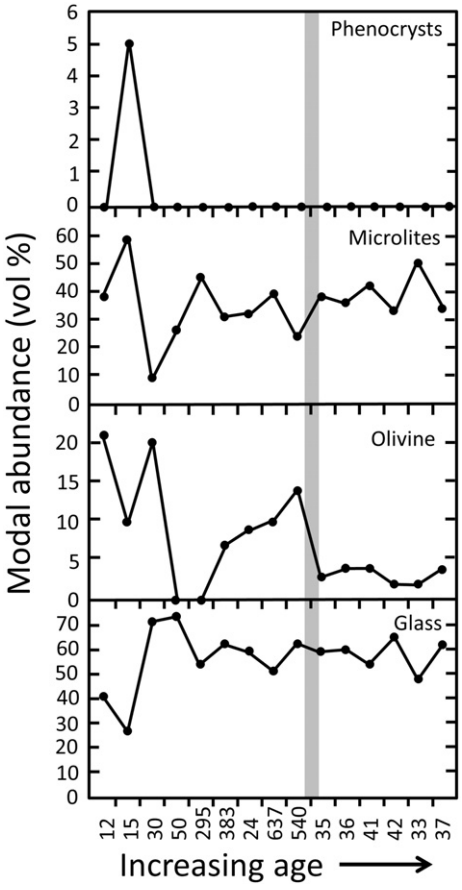

Fig. 7. The modal abundances of phenocrysts, microlites, olivine, and glass in the present samples, plotted in order of increasing age. The grey vertical bar separates the <20 ka samples (to the left) from the >20 ka samples.

Table 4
Literature data for the bulk composition of the geological units from which the present basalts were collected (wt%)[a]. Also listed are normative values for anorthite in plagioclase calculated by the CIPW procedure and forsterite in olivine calculated using the MELTS program (both mol%).

Sample	Unit(N)[b]	SiO_2	TiO_2	Al_2O_3	Fe_2O_3	FeO[c]	MnO	MgO	CaO	Na_2O	K_2O	P_2O_5	CO_2	H_2O	Total	An	Fo
May-12/May-15	p5(21)	50.08	2.62	13.02	11.93	11.26	0.17	8.64	11.03	2.14	0.47	0.26	0.02	0.04	101.05	0.56	0.75
May-50	p4y(29)	51.24	2.82	13.33	9.65	11.43	0.17	6.95	10.13	2.42	0.55	0.33	0.02	0.18	100.64	0.52	0.80
MLO-295/MLO-383	k(21)	50.77	2.10	13.37	6.17	11.04	0.17	8.22	10.02	2.26	0.39	0.26	0.03	0.68	99.85	0.55	0.83
May-30/May-24/MLO-637	k1y(32)	51.00	2.08	13.04	10.19	10.97	0.17	8.96	10.11	2.18	0.37	0.25	0.01	0.23	100.46	0.56	0.82
MLO-540	k10(40)	49.69	1.80	11.85	6.03	11.15	0.17	12.72	9.10	1.86	0.28	0.22	0.03	0.54	100.00	0.58	0.86
May-33	hwt(1)	59.10	0.95	17.80	5.72	5.09	0.19	1.18	2.59	6.60	3.49	0.62	0.01	1.56	99.81	0.13	0.65
May-36	hwb(18)	55.53	1.57	17.83	8.22	7.31	0.22	1.97	3.86	5.81	2.78	0.91	0.00	0.95	99.65	0.20	0.69
May-35/May-41	hw(78)	49.51	2.51	17.13	11.51	10.24	0.24	3.44	6.01	4.78	1.91	1.68	0.01	1.26	100.00	0.31	0.74
May-37	pi(111)	48.20	3.22	14.79	13.57	12.08	0.19	6.15	9.91	2.90	0.85	0.50	0.01	0.45	100.75	0.49	0.79

[a] Bulk compositions from Wolfe and Morris (1996), An and Fo this work.
[b] "Unit" refers to the geological unit on the map of Wolfe and Morris (1996). N is the number of analyses.
[c] All Fe expressed as FeO.

4. Discussion

4.1. TL sensitivity and age

The young age samples (<20 ka) from Kilauea group in a fairly tight cluster on a plot of log TL against age (Fig. 5), setting aside MLO295 which seems to be a low outlier. The ~150–200 ka samples from Kohala plot in a lose cluster at about an order of magnitude higher values TL values. In fact, a regression line passes through the two clusters, making essentially a two point correlation between log TL and age. Importantly, the lone 400 ka sample from Kohala plots well off the regression line. While the correlation is not strong, what is noteworthy is the disagreement between the present correlation and the correlation shown by the Idaho samples. Also important is that the 400 ka sample approaches the Idaho line, so that the Idaho line might better be termed the "tholeiite line". This difference in the induced TL of the tholeiites and the induced TL of the alkali basalts is to be expected in view of their major compositional difference, especially with respect to feldspar composition.

4.2. Differences in feldspar composition

The study of Benoit et al. (2001) showed that there was a strong dependence of the induced TL of feldspars on composition (Fig. 9). As the anorthite content increases from zero to 100% the induced TL decreases by over three orders of magnitude. A line fitted to the data has the equation:

$$\text{Log (TL sens)} = -0.0316\,\text{An} + 4.3125 \quad (1)$$

where the induced TL is in units of Dhajala = 1000 (and termed "TL sensitivity") and An is in mol%. The R^2 value is 0.986. Given the range of normative feldspar composition we have in these samples, this must explain much of the spread in the induced TL values observed.

We can use this equation to correct for differences in feldspar composition, normalizing all our data to an arbitrary value of An_{48}. The plot of induced TL against age now appears quite different with the alkali basalts lying more-or-less on the same line as the tholeiitic basalts (Fig. 10). R^2 values for the two trend lines are indicated on the diagram, and details of the data used to produce Fig. 10, with the complete line analyses, are given for both sites in Appendix.

The TL-age plot for Hawaii (Fig. 10) can now be compared with the equivalent plot for Idaho (Fig. 1) and to aid the comparison the regression line from Fig. 1 has been included in Fig. 10. Again, no data have been weighted, none ignored, and the data are fitted to the raw data as plotted in Fig. 10. Details appear in the Appendix. The slope for the Hawaii data is about half that for the Idaho data (0.0015 ± 0.0012 for Hawaii cf. 0.0039 ± 0.0014 for Idaho, 2σ uncertainties) but given the uncertainties, the difference may not be significant. It is even possible that the slope on the Hawaii data is zero. However, it is clear that the reason for the difference in slope is the behavior of the data for samples <50,000 years old. Consistent with this, the intercepts do not overlap (0.78 ± 0.18 for Hawaii cf. -0.079 ± 0.28 for Idaho, 2σ uncertainties). In both cases there is an order of magnitude spread, but data for Idaho basalts is skewed to lower values than the data for the Hawaii samples which are tightly clustered near the top of the range. The value for MLO-295, which we have been considering an outlier, is now seen to

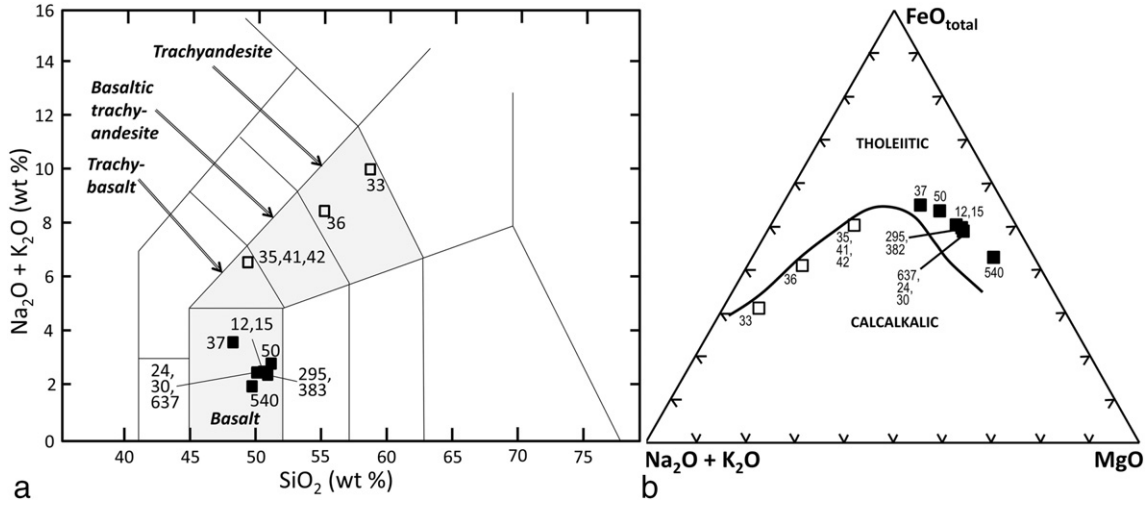

Fig. 8. (a) Compositional data for the present samples plotted on a total alkali against silica plot. Most of the present samples are basalts, or basalt-like, although five are high in alkalis and silicon and appear in the trachybasalt and trachyandesite fields. (b) Alkali-FeO-MgO plot for the present samples showing that while most of the samples are tholeiitic, five are high in alkalis.

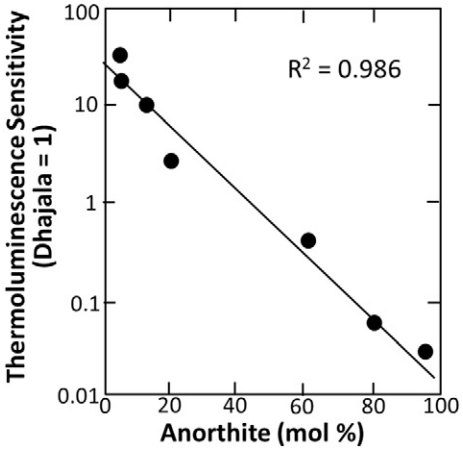

Fig. 9. Induced thermoluminescence plotted against anorthite content for a suite of pure feldspars. Figure produced from data in Benoit et al. (2001).

be similar to many of the low TL Idaho samples. To understand these data, especially if we are to have any chance of finding a new method for chronology, it is essential to understand why the young basalts show such a large range of induced TL values and why the Hawaii samples differ from the Idaho samples.

4.3. Primary versus secondary feldspar

We suggest that a major factor causing the variations in induced TL is the relative amount of luminescent feldspar in (1) the lavas at the time they formed (i.e. brought up with the lava and solidified in the flow) and (2) produced by solid state effects after solidification. The time period associated with step (2) is the "age" of the samples. We refer to feldspar formed in these two ways as (1) "primary" and (2) "secondary". Differences in the amount and composition of "primary" feldspar would account for the differences we see in the basalts from Idaho and Hawaii.

We can find no evidence in the petrographic data for the ratio of primary to secondary feldspar playing a major part in the induced TL properties of these basalts. This conclusion applies to the spread in the TL sensitivity of the young basalts and with the TL trends for the older

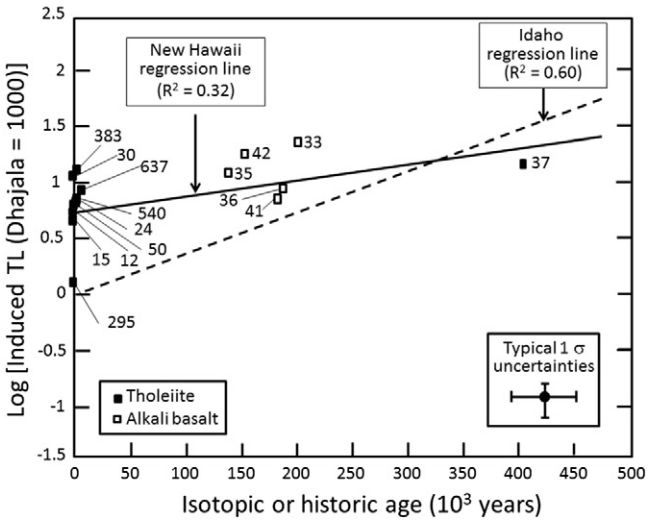

Fig. 10. Plot of the log of the composition corrected induced TL of the present basalt samples against isotopic of historic age. The correlation is weak but now the Hawaii tholeiites plot on the same line as the alkali basalts. Also shown is the regression line for basalts (predominantly tholeiites) from the eastern Snake River Plain in Idaho which has a steeper slope. For comments on typical uncertainties see the caption to Fig. 1.

samples. In fact, we only observed phenocrysts in one of our samples, and certainly there was no relationship between phenocrysts and distance away from the trend line; sample 15 is the only sample with measurable phenocryst content (Fig. 6) plots with the low-age samples in Figs. 5 and 10. In comparing the modal phase abundance for young basalts at Idaho and Hawaii, the only significant difference is the higher olivine content of the Hawaii basalts (say 5–20%) compared to the Idaho basalts (generally ~0%).

Based on thermodynamic equilibrium calculations using the alphaMELTS algorithm (Ghiorso and Sack, 1995; Smith and Asimow, 2005), predicted forsterite content across our sample suite cluster around $Fo_{78 \pm 06}$ at the highest temperature, and become more iron-rich toward lower temperatures. Olivines of the bulk composition observed here do not luminesce, so this should not affect the induced TL data.

The location of peaks in the TL glow curves (Fig. 3) suggests that the minerals present are essentially common to all samples, but says nothing about amount. The specimen glow curves shown in Fig. 3 might provide further insight into the mineralogy with respect to primary and secondary phases. The "atypical" curves stood out sharply during TL measurement because of their unusual nature and they were checked several times. Only after preparing Fig. 3 was it realized that all of the atypical samples were young in age. It could be that zero age, freshly erupted samples have the mineralogy of samples May-12, May-15, and MLO-295 and that the broad lower temperature TL characteristic of "typical" samples was produced subsequent to eruption. This would be consistent with our current ideas regarding the phases that are responsible for these TL peaks; ~300 °C due to calcic phases (such as anorthite), ~200 °C peak due to high-temperature plagioclase and ~100 °C peak due to low-temperature plagioclase. However, the data are, at the moment, only suggestive and no trend between peak shape and age was observed for the Idaho basalts.

4.4. Induced TL and weathering of basalts

Fig. 11 summarizes the two major climatic parameters (temperature and precipitation) for Craters of the Moon, Kilauea Point and Kohala Mission. The annual precipitation in Idaho is considerably lower than in Hawaii and temperatures are uniformly higher in Hawaii but show strong seasonal variation in Idaho, reaching Hawaii-like values for only a short period each year. Despite these climatic differences, we do not think weathering is affecting our data. Our samples were chosen to be free of weathering products and there was no evidence for weathering products in the thin sections of our samples. The same was true of our Idaho study.

4.5. So where do we stand as a dating method?

At this point we do not claim we have a dating method, simply a possible mechanism that might lead to a dating method in the event that we were able to remove the scatter and quantify the processes. However, we summarize our current status in Fig. 12 which takes the regression lines from Fig. 10 and the typical uncertainties quoted in the same figure and draws two "trend lines", one for Idaho and one for Hawaii. It can be seen that an induced TL of ten would lead us to suggest an age for the Hawaii samples of 150 ± 100 ka while an induced TL of three would lead us to an age of 150 ± 50 ka for the Idaho samples. (We stagger these two TL values to clarify their plotting on Fig. 12). Clearly, the slope is critical to determining the uncertainty in our age estimates and this is governed mostly by the low-age samples. However, in a sense Fig. 12 is misleading in terms of the future prospects of induced TL dating. The uncertainty on our lines depends mostly on the uncertainty in the radiometric ages and the accuracy of the TL values; the precision on the individual TL measurements is 20% and about the size of the symbols on a log plot. We can remove reliance on radiometric ages with their relatively large uncertainties by performing kinetic studies on the induced TL signal in the laboratory and thus obtain an

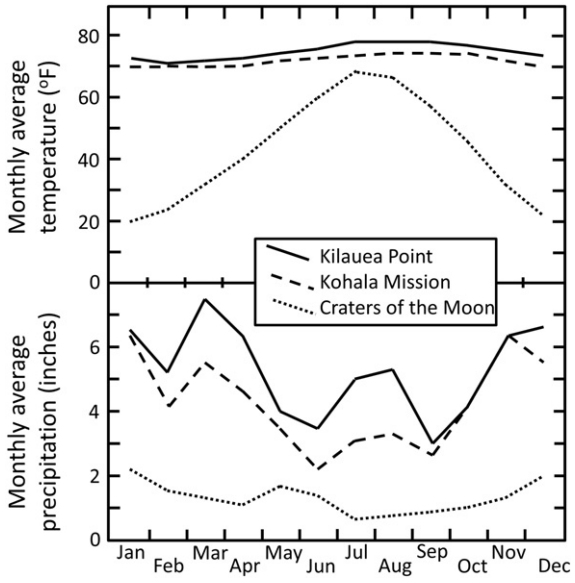

Fig. 11. Monthly average temperature and precipitation at Kilauea Point and Kohala Mission in Hawaii and Craters of the Moon in Idaho. Data from the Western Regional Climate Center (http://www.wrcc.dri.edu/climatedata/comparative/ accessed July 30th, 2016).

absolute method of dating by induced TL. This is straight-forward. Removing the scatter in the low-age samples is another challenge and our next step in that process is to explore the variation along single flows. We currently have samples of single flows from Idaho and Hawaii.

5. Conclusions

The basalts of the Big Island of Hawaii show a weak correlation between the log of the composition-corrected induced TL and the historic and radiometric ages of the samples. The TL parameter increases with age as we predicted and previously observed by May (1977, 1979).

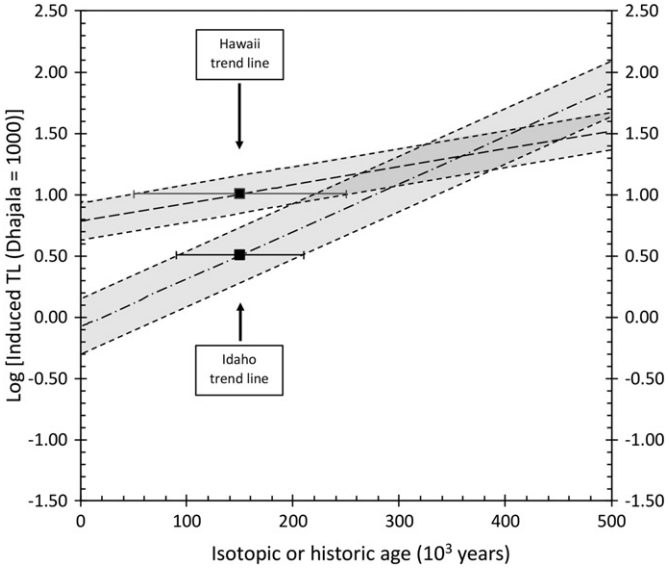

Fig. 12. Summary of the present situation with respect to dating uncertainties. Using the statistical parameters shown in the Appendix, we find the slopes and 2σ uncertainty envelopes indicated above. For an induced TL of 10, the Hawaii line plus envelope gives an age of about 150 ± 100 ka while an induced TL of three and the Idaho line plus envelope gives us an age of 140 ± 60 ka. These TL values were staggered to clarify the diagram; an induced TL of ten gives 270 ± 60 ka on the Idaho line.

The slope for the Hawaii data is shallower than in case for the Idaho samples because of differences in the TL data for the youngest samples (<50,000 years). While young basalts in both Idaho and Hawaii show a similar range of TL values, when outliers are included, the Hawaii data are skewed to higher values. The reason is unclear, but this will be the next topic to explore if this technique is to stand any chance of being a useful chronometer. We can find no evidence that the proportion of primary and secondary feldspar is affecting the data, and weathering effects do not appear to be important. These results provide a further indication that the induced TL method might ultimately have application as a chronometer, provided the causes of the scatter can be identified and a means found for correcting them. Future plans are to (1) investigate the cause of the spread in TL values among samples with <50,000 year ages by measuring the induced TL properties of basalts along single flows at both Hawaii and Idaho, and (2) determine the kinetics of these processes by laboratory measurements which would put the induced TL dating method on an absolute footing.

Acknowledgements

We appreciate help of Jennifer Heldmann, PI of the FINESSE node of SSERV Institute, for financial support, members of the FINESSE team for help with sample collection, and Darlene Lim, PI of the BASALT project, for essential logistical support. Reviews by the Editor and two external reviewers are also appreciated.

Appendix

Age, log (TL)[a], and line analysis data for the Hawaii and Idaho volcanic fields.

Hawaii	Age	log TL_{uncorr}	log TL_{corr}	Idaho	Age	log TL_{uncorr}	log TL_{corr}
May-12	0.075	0.45	0.70	BLU	2.076	0.04	−0.40
May-15	0.085	0.48	0.73	HHA	5.2	−0.40	−0.30
May-30	0.156	0.80	1.05	BCB	6.02	0.38	−0.63
May-50	0.265	0.52	0.64	LTP	6.5	0.49	−0.24
MLO-295	1.3	−0.15	0.07	CAK	6.6	0.23	0.36
MLO-383	3.5	0.89	1.11	GRAA	7.36	0.66	0.25
24-May	3.74	0.54	0.80	GRAB	7.36	0.26	−1.26
MLO-637	3.9	0.58	0.83	NOR	11.6	0.23	0.48
MLO-540	8	0.58	0.90	SUN	12.01	0.49	−0.30
May-35	140	1.63	1.09	CAR	12.01	0.15	−0.33
May-33	153	2.37	1.26	SPU	57	0.58	0.20
May-36	181	1.74	0.86	QUA	64	0.04	0.52
May-41	184	1.48	0.95	STB	113	1.14	1.27
May-42	196	1.92	1.38	BLO	116	1.18	0.81
May-37	400	1.18	1.21	WAG	120	1.12	0.74
				SER	120	0.63	0.82
				PRA	263	0.63	0.82
				MOS	265	0.54	0.73
				PAC	340	0.85	1.14
				CED	400	1.31	1.65
				BPL	430	1.75	2.04
				ANT	470	0.89	0.89

Line analysis[b]				
Slope	0.0038	0.0015	0.0022	0.0039
Slope σ	0.0012	0.0006	0.0005	0.0007
Intercept	0.67	0.78	0.32	−0.079
Intercept σ	0.17	0.09	0.10	0.14
R^2	0.43	0.31	0.47	0.60
Std. error (y)	0.54	0.27	0.10	0.51
F factor	10.02	5.72	18	30.3
DOF	13	13	20	20
SS (reg)[c]	2.91	0.43	2.45	7.82
SS (res)[d]	3.78	0.98	2.73	5.16
RMSE[e]	0.38	0.19	0.29	0.40

[a] TL_{uncorr} refers to TL data before correction for compositional variations, TL_{corr} refers to TL data that have been corrected for compositional variations.

[b] As per Excel LINEST software.

[c] Sum of squares (regression).

[d] Sum of squares (residuals).

[e] RMSE: 1σ Root-mean-square error between the y-values of induced TL to the y-value from the linear regression.

References

Aitken, M.J., 1985. Thermoluminescence Dating. Academic Press, Orlando, USA (359 pp.).

Aitken, M.J., 1999. Introduction to Optical Dating. Oxford University Press, Oxford, UK (280 pp.).

Akridge, D.G., Akridge, J.M.C., Batchelor, J.D., Benoit, P.H., Brewer, J., DeHart, J.M., Keck, B.D., Jie, Lu, Meier, A., Penrose, M., Schneider, D.M., Sears, D.W.G., Symes, S.J.K., Yanhong, Zhang, 2004. Photomosaics of the cathodoluminescence of 60 sections of meteorites and lunar samples. J. Geophys. Res. Vol. 109 (Issue E7) (CiteID E07S03).

Batchelor, J.D., Sears, D.W.G., 1991a. Metamorphism of eucrite meteorites studied quantitatively using thermoluminescence. Nature 349, 516–519.

Batchelor, J.D., Sears, D.W.G., 1991b. Thermoluminescence constraints on the metamorphic, shock and brecciation history of basaltic meteorites. Geochim. Cosmochim. Acta 55, 3831–3844.

Benoit, P.H., Hartmetz, C.P., Batchelor, D.J., Symes, S.J.K., Sears, D.W.G., 2001. The induced thermoluminescence and thermal history of plagioclase feldspars. Am. Mineral. 76, 780–789.

Berger, G.W, 1991. The use of glass for dating volcanic ash by thermoluminescence. J. Geophys. Res 96, 19705–19720.

Drake, M.J., 2001. The eucrite/Vesta story. Meteorit. Planet. Sci. 36 (4), 501–513.

Ghiorso, M.S., Sack, R.O., 1995. Chemical mass transfer in magmatic processes IV. A revised and internally consistent thermodynamic model for the interpolation and extrapolation of liquid-solid equilibria in magmatic systems at elevated temperatures and pressures. Contrib. Mineral. Petrol. 119:197–212. https://doi.org/10.1007/BF00307281.

Guérin, G., Valladas, G., 1980. Thermoluminescence dating of volcanic plagioclases. Nature 286, 697–699.

Lalou, C., Nordemann, D., Labyrrie, J., 1970. Etude préliminaire de la thermoluminescence de la meteorite. Saint-Severin. CR Acad. Sci. Paris 2401 Ser. D 270.

May, R.J., 1977. Thermoluminescence dating of Hawaiian alkalic basalts. JGR 82, 3023–3029.

May, R.J., 1979. Thermoluminescence dating of Hawaii basalt. Geol. Surv. Prof. Paper 1095.

McCord, T.B., Adams, J.B., Johnson, T.V., 1970. Asteroid vesta: spectral reflectivity and compositional implications. Science 168, 1445–1447.

McDougall, I., 1969. Potassium-argon ages on lavas of Kohala Volcano, Hawaii. Geol. Soc. Am. Bull. 80, 2597–2600.

McDougall, I., Swanson, D.A., 1972. Potassium-argon ages of lavas from the Hawi and Pololu Volcanic Series, Kohala Volcano, Hawaii. Geol. Soc. Am. Bull. 83, 3731–3738.

Rubin, M., Corrine, A., 1960. U.S. Geological Survey radiocarbon dates V. Am. J. Sci. Radiocarbon Supp. vol. 2, 129–185.

Sears, D.W.G., 2015. Induced thermoluminescence dating of basalts. Ancient TL 33, 15–19.

Sears, D.W., Grossman, J.N., Melcher, C.L., Ross, L.M., Mills, A.A., 1980. Measuring the metamorphic history of unequilibrated ordinary chondrites. Nature 287, 791–795.

Sears, D.W.G., Ninagawa, K., Singhvi, A.K., 2013. Luminescence studies of extraterrestrial materials: insights into their recent radiation and thermal histories and into their metamorphic history. Chem. Erde 73, 1–37.

Sears, D.W., Sears, H., Sehlke, A., Hughes, S.S., 2017. Induced thermoluminescence as a method for dating recent volcanism: eastern Snake River Plain, Idaho, USA. J. Geophys. Res. Solid Earth 122, 906–922.

Smith, P.M., Asimow, P.D., 2005. Adiabat_1ph: a new public front-end to the MELTS, pMELTS, and pHMELTS models. Geochem. Geophys. Geosyst. 6:Q02004. https://doi.org/10.1029/2004GC000816.

Sullivan, B.M., Spiker, E., Rubin, M., 1970. U.S. geological survey radiocarbon dates XI. Radiocarbon 12, 319–334.

Sutton, S.R., 1985. Thermoluminescence measurements on shock-metamorphosed sandstone and dolomite from meteor crater, Arizona. I - shock dependence of thermoluminescence properties. II thermoluminescence age of meteor crater. J. Geophys. Res. 90, 3683–3700.

Wintle, A.G., 1973. Anomalous fading of thermoluminescence in mineral samples. Nature 245, 143–144.

Wolfe, E.W., Morris, J., 1996. Geologic Map of the Island of Hawaii. Miscellaneous Investigations Series, Map I-2524-A and Sample Data for the Geologic Al Map of the Island of Hawaii, Brochure to Accompany Map.